J|A|C|S
ARTICLES
Published on Web 11/18/2006

Aggregation-Mediated Optical Properties of pH-Responsive Anionic Conjugated Polyelectrolytes

Fuke Wang and Guillermo C. Bazan*

Department of Materials and Chemistry & Biochemistry, Institute for Polymers and Organic Solids, University of California, Santa Barbara, California 93106

Received July 16, 2006; E-mail: bazan@chem.ucsb.edu

Abstract: Conjugated polyelectrolyte copolymers containing 2,1,3-benzothiadiazole- (BT) and oligo(ethylene oxide)-substituted fluorene and phenylene units have been designed and synthesized. The phenylene pendent groups also have carboxylic acid functionalities, which allow probing the effect of pH on optical properties. The BT content in the backbone can be regulated at the synthesis stage. Dynamic light scattering studies show that polymers aggregate in water at low pH. Increased interchain contacts give rise to a lowering of the photoluminescence (PL) efficiency via self-quenching when the BT units are absent and increased levels of FRET from the phenylene−fluorene segments to BT. Furthermore, the PL efficiency of BT increases in the aggregated structures. Examination of solvent effects indicates that the increased BT efficiencies are likely due to decreased contact with water. The changes in PL efficiencies are reversible, showing that the aggregates are dynamic and not kinetically constrained.

Introduction

The delocalized electronic structure of π-conjugated polymers allows for effective coupling between optoelectronic segments.[1] Properties such as charge transport,[2] conductivity,[3] emission efficiency,[4] and exciton migration[2] are easily perturbed by external agents, leading to large changes in measurable signals.[5] Trace detection of analytes has been successfully accomplished by making use of these amplification mechanisms.[4,6,7] Conjugated polyelectrolytes (CPs) are conjugated polymers with pendent functionalities capable of ionizing in high dielectric media. Their solubility in water makes them appropriate for interrogation of biological targets in aqueous media.[4,7,8] These water-soluble materials have been used as light-harvesting molecules that deliver excitations upon recognition events to signaling fluorophores attached to biomolecular probes, thereby providing signal intensities above those of single-molecule reporters.[5,9] Nonspecific contacts between nontarget species and the hydrophobic CP backbone are complex and need special attention for attaining selectivity as these interactions can easily lead to misinterpretation of results.[10]

Differences in the efficiencies of intra- and interchain Förster resonance energy transfer (FRET) have been used to design CPs with optical signatures that are sensitive to DNA concentration.[11] Interchain FRET is more effective as a result of more effective

(1) (a) Guillet, J. E. *Polymer Photophysics and Photochemistry*, Cambridge University Press: Cambridge, 1985. (b) Weber, S. E. *Chem. Rev.* **1990**, *90*, 1469. (c) Kauffmann, H. F. *Photochemistry and Photophysics*; Radek, J. E., Ed.; CRC: Boca Raton, 1990; Vol 2. (d) Scholes, G. D.; Ghiggino, K. P. *J. Chem. Phys.* **1994**, *101*, 1251. (e) Tasch, S.; List, E. J. W.; Hochfilzer, C.; Leising, G.; Schlichting, P.; Rohr, U.; Geerts, Y.; Scherf, U.; Mullen, K. *Phys. Rev. B* **1997**, *56*, 4479. (f) Nguyen, T. Q.; Wu, J. J.; Doan, V.; Schwartz, B. J.; Tolbert, S. H. *Science* **2000**, *288*, 652. (g) Pschirer, N. G.; Byrd, K.; Bunz, U. H. F. *Macromolecules* **2001**, *34*, 8590. (h) Beljonne, D.; Pourtois, G.; Silva, C.; Hennebicq, E.; Herz, L. M.; Friend, R. H.; Scholes, G. D.; Setayesh, S.; Müllen, K.; Brédas, J. L. *Proc. Natl. Acad. Sci. U.S.A.* **2002**, *99*, 10982. (i) Liu, B.; Wang, S.; Bazan, G. C.; Mikhailovsky, A. *J. Am. Chem. Soc.* **2003**, *125*, 13306. (j) Liu, B.; Bazan, G. C. *J. Am. Chem. Soc.* **2004**, *126*, 1942.
(2) Lee, D. W.; Swager, T. M. *Synlett* **2004**, 149.
(3) (a) Korri, Y. H.; Garnier, F.; Srivastava, P.; Godillot, P.; Yassar, A. *J. Am. Chem. Soc.* **1997**, *119*, 7388. (b) Bäuerle, P.; Emge, A. *Adv. Mater.* **1998**, *10*, 324. (c) Garnier, F.; Korri, Y. H.; Srivastava, P.; Mandrand, B.; Delair, T. *Synth. Met.* **1999**, *100*, 89. (d) Korri. Y. H.; Yassar, A. *Biomacromolecules* **2001**, *2*, 58.
(4) (a) Chen, L.; McBranch, D. W.; Wang, H.; Helgeson, R.; Wudl, F.; Whitten, D. *Proc. Natl. Acad. Sci. U.S.A.* **1999**, *96*, 12287. (b) Kumaraswamy, S.; Bergstedt, T.; Shi, X.; Rininsland, F.; Kushon, S.; Xia, W. S.; Ley, K.; Achyuthan, K.; McBranch, D.; Whitten, D. *Proc. Natl. Acad. Sci. U.S.A.* **2004**, *101*, 7511. (c) Pinto, M. R.; Schanze, K. S. *Proc. Natl. Acad. Sci. U.S.A.* **2004**, *101*, 7505.
(5) Swager, T. M. *Acc. Chem. Res.* **1998**, *31*, 201.
(6) (a) Yang, J. S.; Swager, T. M. *J. Am. Chem. Soc.* **1998**, *120*, 11864. (b) Yang, J. S.; Swager, T. M. *J. Am. Chem. Soc.* **1998**, *120*, 5321. (c) Leclerc, M. *Adv. Mater.* **1999**, *11*, 1491. (d) McQuade, D. T.; Pullen, A. E.; Swager, T. M. *Chem. Rev.* **2000**, *100*, 2537. (e) Ewbank, P. C.; Nuding, G.; Suenaga, H.; McCullough, R. D.; Shinkai, S. *Tetrahedron Lett.* **2001**, *42*, 155. (f) Ho, H. A.; Boissinot, M.; Bergeron, M. G.; Corbeil, G.; Doré, K.; Boudreau, D.; Leclerc, M. *Angew. Chem., Int. Ed.* **2002**, *41*, 1548. (g) Kim, I. B.; Erdogan, B.; Wilson, J. N.; Bunz, U. H. F. *Eur. J. Chem.* **2004**, *10*, 6247. (h) Rose, A; Zhu, Z. G.; Madigan, C. F.; Swager, T. M.; Bulovic, V. *Nature* **2005**, *434*, 876. (i) Kim, I. B.; Dunkhorst, A.; Gilbert, J.; Bunz, U. H. F. *Macromolecules* **2005**, *38*, 4560. (j) Kim, I. B.; Wilson, J. N.; Bunz, U. H. F. *Chem. Commun.* **2005**, *10*, 1273.
(7) (a) DiCesare, N.; Pinto, M. R.; Schanze, K. S.; Lakowicz, J. R. *Langmuir* **2002**, *18*, 7785. (b) Liu, B.; Bazan, G. C. *Chem. Mater.* **2004**, *16*, 4467. (c) Leclerc, M.; Ho, H. A. *Synlett* **2004**, *2*, 380. (d) Le Floch, F.; Ho, H. A.; Harding, L. P.; Bedard, M.; Neagu, P. R.; Leclerc, M. *Adv. Mater.* **2005**, *17*, 1251. (e) Ho, H. A.; Bers-Aberem, M.; Leclerc, M. *Eur. J. Chem.* **2005**, *11*, 1718. (f) Nilsson, K. P. R.; Inganäs, O. *Nat. Mater.* **2003**, *2*, 419. (g) Nilsson, K. P. R.; Olsson, J. D. M.; Stabo-Eeg, F.; Lindgren, M.; Konradsson, P.; Inganäs, O. *Macromolecules* **2005**, *38*, 6813. (h) Herland, A.; Nilsson, K. P. R.; Olsson, J. D. M.; Hammarstrom, P.; Konradsson, P.; Inganäs, O. *J. Am. Chem. Soc.* **2005**, *127*, 2317.
(8) (a) Pinto, M. R.; Schanze, K. S. *Synthesis-Stuttgart* **2002**, *9*, 1293. (b) Traser, S.; Wittmeyer, P.; Rehahn, M. *e-polymer* **2002**, 032.
(9) (a) McQuade, D. T.; Hegedus, A. H.; Swager, T. M. *J. Am. Chem. Soc.* **2000**, *122*, 12389. (b) Gaylord, B. S.; Heeger, A. J.; Bazan, G. C. *Proc. Natl. Acad. Sci. U.S.A.* **2002**, *99*, 10954. (c) Kim, T. H.; Swager, T. M. *Angew. Chem. Int. Ed.* **2003**, *42*, 4803. (d) Gaylord, B. S.; Heeger, A. J.; Bazan, G. C. *J. Am. Chem. Soc.* **2003**, *125*, 896.
(10) Dwight, S. J.; Gaylord, B. S.; Hong, J. W.; Bazan, G. C. *J. Am. Chem. Soc.* **2004**, *126*, 16850.
(11) Hong, J. W.; Henme, W. L.; Keller, G. E.; Rinke, M. T.; Bazan, G. C. *Adv. Mater.* **2006**, *18*, 878.

10.1021/ja065061x CCC: $33.50

Scheme 1. Preparation of **P1-BT$_x$**[a]

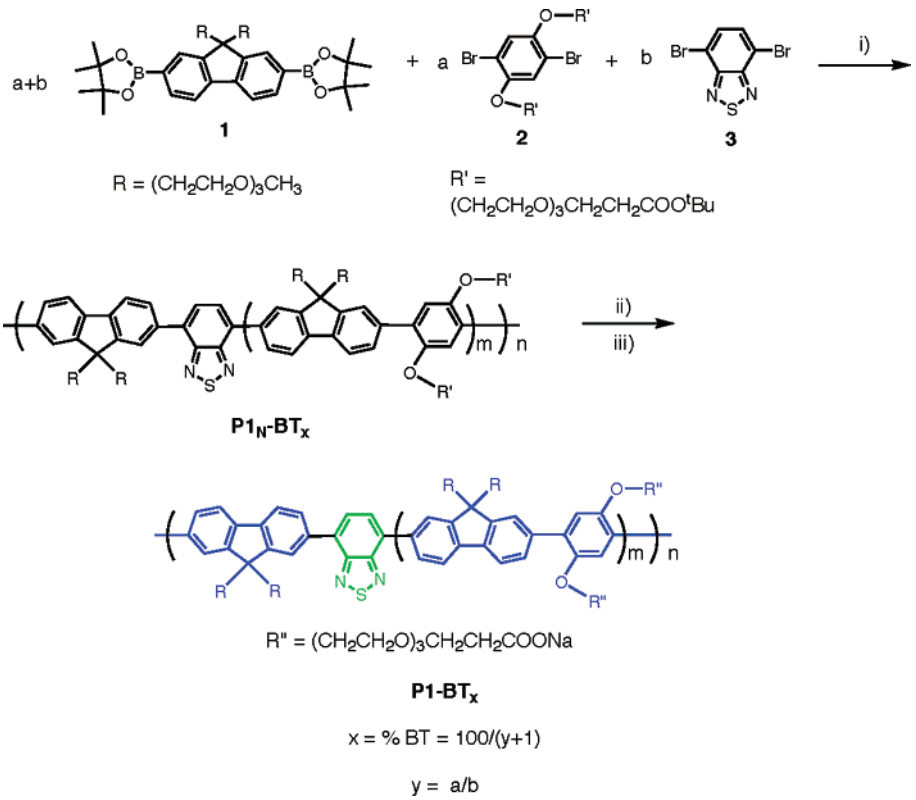

[a] Conditions: (i) 2 M Na_2CO_3, toluene, $Pd(PPh_3)_4$, reflux 48 h; (ii) TFA/CH_2Cl_2 (v/v = 1/1); (iii) Na_2CO_3 (aq).

electronic coupling[12] and the increased dimensionality of the multichromophore system.[13,14] For example, under dilute conditions where multichain aggregation is negligible, emission of poly((9,9-bis(6′-*N*,*N*,*N*,-timethylammoniumbromide)hexyl)-fluorene-*co*-*alt*-1,4-phe nylene-*co*-*alt*-4,7−2,1,3,-benzothiadiazole (**PFPB**) containing 7% 2,1,3,-benzothiadiazole (BT) units (**PFPB$_7$**) occurs in the blue region of the spectrum (390−500 nm). Concentrated solutions emit with a green color characteristic of the BT sites. The working hypothesis is that under these

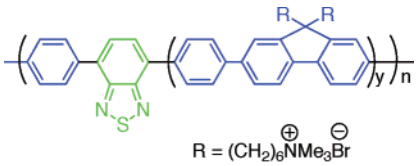

PFPB$_x$ x = % BT = 100/(y+1)

PFPB$_7$ x = 7 = 100/(y+1); y = 93/7

conditions there is an increase of interchain contacts and FRET from the fluorene−phenylene repeat units to the BT sites is more efficient, relative to the situation where chains are more isolated. Addition of a negatively charged polyelectrolyte (such as DNA) induces interpolymer complexation,[15] leading to an increase of the local **PFPB$_7$** concentration, and a shift from the blue-emitting fluorene−phenylene units to the green-emitting BT is observed. It is possible to treat these spectral changes to obtain linear calibration curves from which [DNA] can be determined.[11]

The collective optical response of conjugated polymers can thus be used to develop chemical and biological detection technologies. Conversely, changes in spectral properties are also useful for interrogating how the environment influences elementary self-assembly processes.[16] These organized structures have clear implications on emerging technologies based on organic semiconductors.[17] In this contribution we disclose the design and synthesis of structurally related water-soluble, negatively charged CPs for which electrostatic interactions typical of polyelectrolytes control FRET and fluorescence-quenching processes. The structural design includes carboxylic acid functionalities pendent to the delocalized backbone that can be charged or neutral, depending on the solution pH. The polymer charge was anticipated to control electrostatic repulsion between chains and thus would lead to different levels of aggregation and average interchain distances.[18] We find the unanticipated result that aggregation also controls the emission efficiency of low-energy sites and propose that this is the result of shielding from water within the aggregate structures.

(12) Hennebicq, E.; Pourtois, G.; Scholes, G. D.; Herz, L. M.; Russell, D. M.; Silva, C.; Setayesh, S.; Grimsdale, A. C.; Müllen, K.; Brédas, J.-L.; Beljonne, D. *J. Am. Chem. Soc.* **2005**, *127*, 4744.
(13) Kuroda, K.; Swager, T. M. *Macromol. Symp.* **2003**, *201*, 127.
(14) Kim, J.; Swager, T. M. *Nature* **2001**, *411*, 1030.
(15) (a) In *Self-Assembling Complexes for Gene Delivery. From Laboratory to Clinical Trial*; Kabanov, A. V., Felgner, P. L., Seymour, L. W., Eds.; John Wiley: Chichester, 1998. (b) Gössl, I.; Shu, L.; Schülter, A. D.; Rabe, J. P. *J. Am. Chem. Soc.* **2002**, *124*, 6860. (c) Wang, Y.; Dubin, P. L.; Zhang, H. *Langmuir* **2001**, *17*, 1670. (d) Bronich, T. K.; Nguyen, H. K.; Eisenberg, A.; Kabanov, A. V. *J. Am. Chem. Soc.* **2000**, *122*, 8339.
(16) (a) Praveen, V. K.; George, S. J.; Varhese, R.; Vijayukamar, C.; Ajayaghosh, A. *J. Am. Chem. Soc.* **2006**, *128*, 7542. (b) Liu, B.; Bazan, G. C. *J. Am. Chem. Soc.* **2006**, *128*, 1188. (c) McCullough, R. D.; Ewbank, P. C.; Loewe, R. S. *J. Am. Chem. Soc.* **1997**, *119*, 633. (d) Balamurugan, S. S.; Batchev, G. B.; Yang, Y.; McCarley, R. L. *Angew. Chem., Int. Ed.* **2005**, *44*, 4872.
(17) Hoeben, F. J. M.; Jonjheijm, P.; Meijer, E. W.; Schenning, A. P. H. J. *Chem. Rev.* **2005**, *105*, 1491.
(18) Pinto, M. R.; Kristal, B. M.; Schanze, K. S. *Langmuir* **2003**, *19*, 6523.

Results and Discussion

Structural Design and Synthesis. Scheme 1 shows the synthesis and structures of the polymers used in these studies. Copolymerization of **1** with a stoichiometric quantity determined by the sum of **2** and 4,7-dibromo-2,1,3-benzothiadiazole (**3**) under Suzuki cross-coupling conditions using $Pd(PPh_3)_4$ and Na_2CO_3 provides the neutral precursor polymers $\mathbf{P1_N\text{-}BT}_x$ in which the BT content (x% relative to phenylene units) is regulated by the ratio of **2** to **3**. 2,7-Bis(4,4,5,5-tetramethyl-1,3,2-dioxaborolan-2-yl)-9,9-di(1-(2-(2-methoxy-ethoxy)ethoxy-)ethyl)fluorene (**1**) was obtained by alkylation of 2,7-dibromofluorene with 1-(2-(2-methoxy-ethoxy)ethoxy)-2-bromoethane, followed by esterification with 2-isopropoxy-4,4,5,5-tetramethyl-1,3,2-dioxaborolane.[19,20] Compound **2** was synthesized from 1,4-dibromohydroquinone by modification of published procedures.[21] The $\mathbf{P1_N\text{-}BT}_x$ polymers are soluble in organic solvents such as chloroform, toluene, and THF and can be purified by repeated precipitation from toluene solutions into methanol. Characterization by NMR spectroscopy and elemental analysis is consistent with the proposed structures. Molecular weight determination by GPC analysis against polystyrene standards shows number-average molecular weights (M_n) for the neutral precursor polymers $\mathbf{P1_N\text{-}BT_0}$ ($x = 0$, i.e., no BT units) and $\mathbf{P1_N\text{-}BT_{15}}$ (15% BT units) of 56K (PDI = 1.7) and 26K (PDI = 1.6), respectively. In general, as the BT content increases, one observes a decrease in average polymer molecular weight. Hydrolysis of the ester groups occurs in a CH_2Cl_2 and trifluoroacetic acid (TFA) mixture (v/v = 1/1) at room temperature. After solvent evaporation, the residue is treated with saturated aqueous Na_2CO_3. The target materials are then purified by dialysis against deionized (DI) water using 1 KD molecular weight cutoff dialysis membranes. Final isolation requires removal of water and drying in a vacuum oven at 50 °C for at least 24 h. ^{1}H NMR spectroscopy in CD_3OD of the product shows no signals in the 1.4−1.5 ppm range, indicating greater than 95% removal of *tert*-butyl groups.

P1-BT$_0$ and **P1-BT$_{15}$** are soluble in methanol or water. In DI water, polymer concentrations of up to 2 mg/mL can be obtained in the pH range from 5 to 12. Aqueous solutions of **P1-BT$_0$** are visibly viscous under these conditions. Similar to previously reported nonionic water-soluble conjugated polymers with ethylene oxide side chains,[22] the neutral form of both polymers (i.e., at pH < 3) is also soluble in water, with concentrations as high as 0.05 mg/mL.

pH-Dependent Aggregation of P1-BT$_0$ and P1-BT$_{15}$. One of the goals of this study is to probe how the pH of the solution influences the optical properties of **P1-BT$_0$** and **P1-BT$_{15}$**. We anticipated that protonation of the carboxylic groups at low pH would render the polymers charge neutral and lead to a decrease in interchain electrostatic repulsion. These conditions would encourage interchain aggregation[18] and thereby perturb elementary photophysical processes, such as FRET and fluorescence quenching. In anticipation of these changes, we probed the degree of aggregation by dynamic light scattering (DLS) techniques.[23]

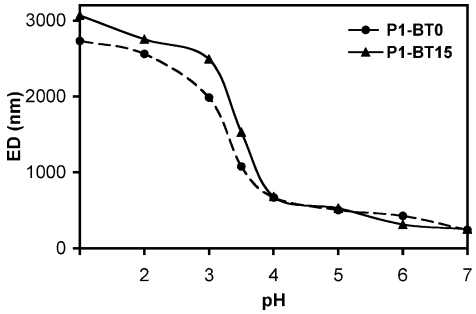

Figure 1. Effective diameter (ED) determined by dynamic light scattering of **P1-BT$_0$** and **P1-BT$_{15}$** ([RU] = 3.8×10^{-5} M) in water as a function of pH.

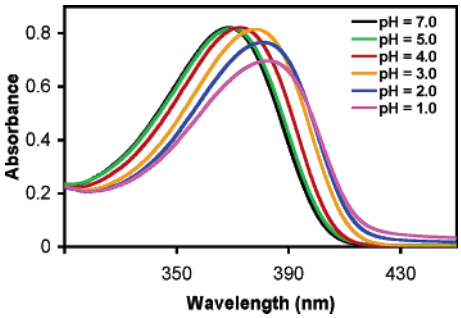

Figure 2. Absorption spectra of **P1-BT$_0$** ([RU] = 3.8×10^{-5} M) in water as the pH is incrementally decreased from 7 to 1.

DLS results in Figure 1 show the effect of pH on the effective diameter (ED) measured from solutions of **P1-BT$_0$** and **P1-BT$_{15}$** in water ([RU] = 3.8×10^{-5} M, RU = polymer repeat unit). At pH > 5 the EDs for the two polymers are in the range of 300−400 nm. As the pH decreases, both polymers show a sudden increase in particle size at pH ≈ 3.5. At pH = 1, **P1-BT$_{15}$** is slightly larger (3000 nm) than **P1-BT$_0$** (2700 nm). These data are in agreement with substantial aggregation of chains occurring upon protonation of pendent groups.

Absorption and Photoluminescence Spectra of P1-BT$_0$ and P1-BT$_{15}$: Effect of pH. Figure 2 shows the absorption spectra of **P1-BT$_0$** in water as a function of pH. For these measurements, the pH of a 20 mL solution ([RU] = 3.8×10^{-5} M) was adjusted with HCl and/or NaOH using a pH meter. Once a stable reading was obtained, 2 mL of the solution was transferred to a cuvette for optical measurements. As shown in Figure 2, the absorption spectra of **P1-BT$_0$** are dominated by the $\pi-\pi^*$ transition. The absorption band becomes broader and the absorption maximum (λ_{max}) red shifts from 370 to 382 nm as the medium becomes more acidic and chains aggregate. For comparison, films of **P1-BT$_0$**, where interchain contacts are maximized, show a λ_{max} of 379 nm. A similar red shift in absorption with aggregation has been observed for other conjugated polyelectrolytes.[18,24] Integration of the absorption bands in Figure 2 allows for a relative comparison of the oscillator strength; only a 5% decrease is observed as the pH decreases from 7 to 1.[25] Thus, neither precipitation nor adsorption of **P1-BT$_0$** to the cuvette walls is a significant process.

(19) Stork, M.; Gaylord, B. S.; Heeger, A. J.; Bazan, G. C. *Adv. Mater.* **2002**, *14*, 361.
(20) Haque, S. A.; Park, T.; Xu, C.; Koops, S.; Schulte, N.; Potter, R. J.; Holmes, A. B.; Durrant, J. R. *Adv. Funct. Mater.* **2004**, *14*, 435.
(21) Wosnick, J. H.; Mello, C. M.; Swager, T. M. *J. Am. Chem. Soc.* **2005**, *127*, 3400.
(22) (a) Matthews, J. R.; Goldoni, F.; Schening, A. P. H. J.; Meijer, E. W. *Chem. Commun.* **2005**, 5503. (b) Disney, M. D.; Zheng, J.; Swager, T. M.; Seeberger, P. H. *J. Am. Chem. Soc.* **2004**, *126*, 13343.
(23) Pecora, R. *Dynamic Light Scattering: Applications of Photon Correlation Spectroscopy*; Plenum Press: New York, 1985.
(24) Wang, S.; Bazan, G. C. *Chem. Commun.* **2004**, 2508.
(25) Li, Y.; Whittle, C. E.; Walters, K. A.; Ley, K. D.; Schanze, K. S. *Pure Appl. Chem.* **2001**, *73*, 497.

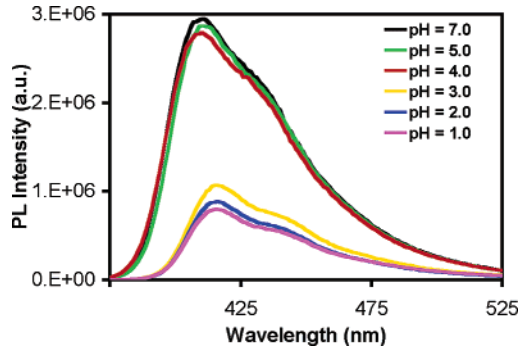

Figure 3. Photoluminescence (PL) spectra of **P1-BT$_0$** ([RU] = 3.8×10^{-5} M) in water as a function of pH (λ_{exc} = 370 nm).

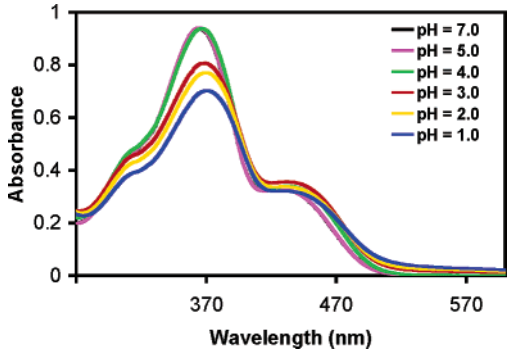

Figure 4. Absorption spectra of **P1-BT$_{15}$** ([RU] = 4.3×10^{-5} M) in water as the pH is incrementally decreased from 7 to 1. Note that the spectra at pH 7.0 and 5.0 overlap each other perfectly.

The photoluminescence (PL) spectra of **P1-BT$_0$** are shown in Figure 3. There is little change in the intensity or shape of the emission band as the pH decreases from 7 to 4. A reduction of 64% in the emission intensity and a slight red shift of the emission maximum (λ_{PL}) from 411 to 416 nm are observed when the pH is lowered from 4 to 3. The PL characteristics then remain essentially unchanged down to pH = 1. The data are consistent with self-quenching upon aggregation at low pH and a red shift in emission as a result of additional interchain delocalization.[26]

Changes induced by the pH on the absorption spectra of **P1-BT$_{15}$** are shown in Figure 4. The absorption of **P1-BT$_{15}$** displays two bands at 364 and 440 nm, which are assigned to the fluorene−phenylene segments and the BT units, respectively.[27] It is interesting to note that relative to **P1-BT$_0$**, the absorption red shift with decreasing pH appears to be less pronounced, although this shift is difficult to quantify because of the overlap between the two transitions. That the absorption spectra of **P1-BT$_{15}$** in Figure 4 are not perturbed by the degree of aggregation suggests that there are no measurable changes in the degree of electronic delocalization in single chains.

The PL spectra of **P1-BT$_{15}$**, with two prominent bands at 410 and 556 nm, are nearly indistinguishable in the pH range from 7 to 4 (Figure 5a). However, decreasing the pH from 4 to 3 results in the disappearance of the high-energy band and in a 7-fold increase of the BT emission intensity at 556 nm. Little change is observed when the pH further decreases to 1. Excitation at 440 nm, where preferential absorption by BT takes

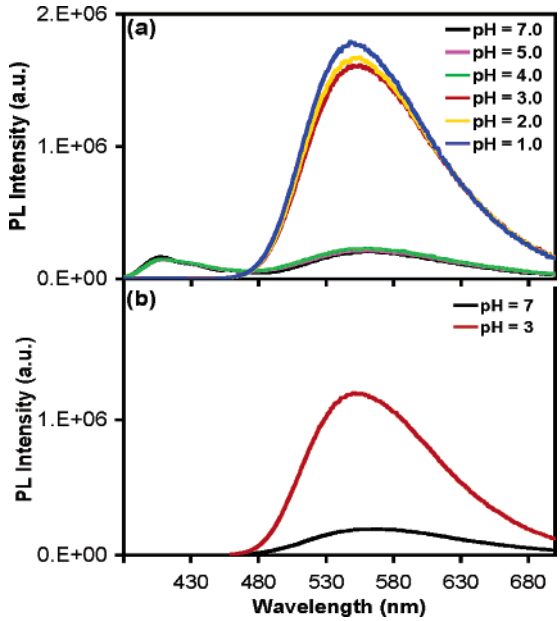

Figure 5. (a) PL spectra of **P1-BT$_{15}$** ([RU] = 4.3×10^{-5} M) in water as a function of pH (λ_{exc} = 370 nm). (b) PL spectra of **P1-BT$_{15}$** ([RU] = 4.3×10^{-5} M) at pH 7 and 3 (λ_{exc} = 440 nm).

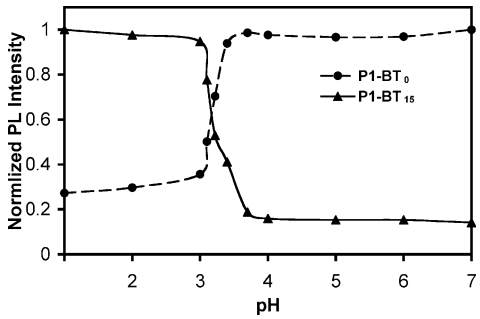

Figure 6. PL response of **P1-BT$_0$** ([RU] = 3.8×10^{-5} M) and **P1-BT$_{15}$** ([RU] = 4.3×10^{-5} M) as a function of pH. Data were normalized relative to the maximum PL intensity of each polymer.

place, yields more intense emission at pH 3 than at pH 7 (Figure 5b). Examination of the excitation spectra by monitoring at 556 nm (Supporting Information) shows that a larger fraction of initial excitations located at fluorene−phenylene sites is capable of sensitizing BT emission at pH = 3 than at pH = 7. Thus, aggregation of **P1-BT$_{15}$** chains results in more effective FRET from the fluorene−phenylene segments to the BT units in an increase in the PL quantum yield of BT.

The pK_a of the pendent carboxylic functionalities can be estimated by looking at 3-[2-(2-(2-hydroxy-ethyoxy)-ethoxy)-ethoxy]propionic acid (HEPA), an analogue of the polymer side chain. The pK_a of HEPA was determined to be 3.7 ± 0.1 by potentiometric titration with 0.1 N NaOH aliquots under nitrogen. Thus, at pH > 3.7, the majority of the pendent groups in **P1-BT$_0$** and **P1-BT$_{15}$** are expected to be deprotonated, yielding the negatively charged chain. Figure 6 shows that the plots of PL emission intensity for **P1-BT$_0$** (λ_{em} = 411 nm) and **P1-BT$_{15}$** (λ_{em} = 556 nm) as a function of pH show a sharp transition in the pH range from 3 to 4. There is an excellent correlation between these data and those in Figure 1, where interchain aggregation occurs within a similar pH range. It is also informative to note that assuming that the inflection point in Figure 1 occurs at the pK_a of the polymer carboxylic groups,

(26) Nguyen, T.-Q.; Martini, I. B.; Liu, J.; Schwartz, B. J. *J. Chem. Phys. B* **2000**, *104*, 237.
(27) Stevens, M. A.; Silva, C.; Russel, D. M.; Friend, R. H. *Phys. Rev. B* **2001**, *63*, 165213.

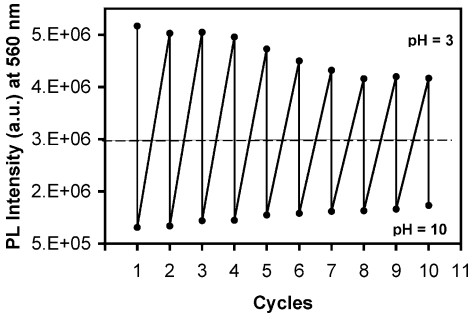

Figure 7. PL intensities at 560 nm of **P1-BT$_{15}$** ([RU] = 4.3×10^{-5} M) upon cycling the pH between 3 and 10.

most of the changes occur within a single pH unit. From eq 1, we see that the aggregation onset begins when less than approximately 75% of the carboxylic groups are deprotonated.

$$\mathrm{pH} - \mathrm{p}K_a = -\log\left[\frac{[\mathrm{HA}]}{[\mathrm{A}^-]}\right] \qquad (1)$$

Changes in the PL spectra as a function of pH are reversible. Figure 7 shows that it is possible to modulate the PL intensity of **P1-BT$_{15}$** ([RU] = 4.3×10^{-5} M) by cycling the pH between 3 and 10. These data indicate that "activating" and "neutralizing" the polymer charge by changing the pH results in reversible aggregation. Furthermore, the time interval between the pH change and PL measurements was on the order of less than 1 min. Thus, aggregate breakup is not kinetically constrained.

Aggregation and Optical Properties of Neutral Precursor Polymers. To summarize the studies on charged polymers in the preceding section, we find that PL self-quenching of **P1-BT$_0$** and the more efficient FRET in the case of **P1-BT$_{15}$** at pH < 4 are well accommodated within the framework provided by more intimate interchain contacts within supramolecular aggregates. A remaining issue is the lower quantum efficiency for BT under basic conditions. To probe the possibility that the increased efficiency is due to the more hydrophobic environment in the aggregated structures we examined the optical properties of the precursor polymers in mixed solvents. The changes in the PL spectra of **P1$_N$-BT$_{15}$** in THF upon addition of water are shown in Figure 8. In contrast to **P1-BT$_{15}$** in basic aqueous media, excitation at 370 or 440 nm in pure THF results in emission that is almost completely BT-based. Thus, excited state initially generated in the fluorene−phenylene segments decay thermally or are transferred to BT sites by FRET. Surprisingly, DLS shows that the ED in these solutions ([RU] = 4.0×10^{-5} M) is ∼2500 nm, much larger than that observed for **P1-BT$_{15}$** at pH = 7. Extensive aggregation of polymer chains in THF therefore occurs at this concentration and is probably driven by stacking of the polarizable π-delocalized backbone. The PL intensity decreases 50% as the water content of in the THF solution increases from 0% to 10%. DLS shows that with 10% water content the effective diameter does not change substantially (∼2400 nm) relative to pure THF. This information shows that there is essentially no difference in the particle size as water is included in the solvent, although changes within the internal structure or the aspect ratio of these aggregates cannot be ruled out. Altogether, these data suggest that the emission efficiency of BT decreases as the water concentration increases, consistent with a charge-transfer excited state that increases its rate of

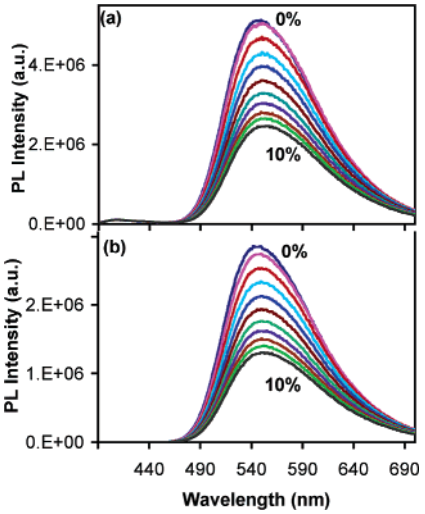

Figure 8. PL spectra of **P1$_N$-BT$_{15}$** ([RU] = 4.0×10^{-5}M) in THF with water content from 0% to 10% in 1% increments: (a) λ_{exc} = 370 nm and (b) λ_{exc} = 440 nm.

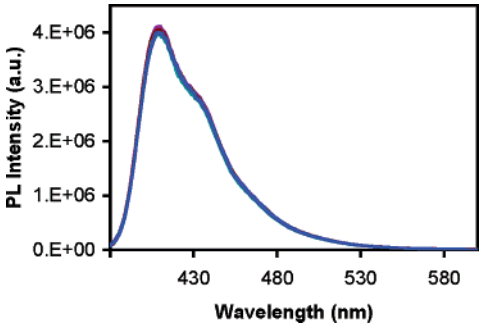

Figure 9. PL spectra (λ_{exc} = 370 nm) change of neutral precursor polymer **P1$_N$-BT$_0$** ([RU] = 4.0×10^{-5} M) in THF with water content from 0% to 10% in 1% increments. The spectra have nearly perfect overlap with each other.

nonradiative deactivation in more polar solvents.[28] The charge-transfer character is also confirmed by the red shift of the PL maximum with increasing water content from 545 nm in pure THF to 554 nm in THF with 10% water. Additionally, from these data we infer that in solutions of **P1-BT$_{15}$** at pH < 4, aggregation introduces the BT units within the interior of the aggregates where water contact is not as pronounced, thereby increasing the emission efficiency.[29]

A similar set of experiments to those illustrated in Figure 8 was done using **P1$_N$-BT$_0$** instead of **P1$_N$-BT$_{15}$**. As shown in Figure 9, there is no change in the PL spectra of **P1$_N$-BT$_0$** in THF upon addition of water up to a total concentration of 10% by volume. DLS measurements show that the aggregate size of **P1$_N$-BT$_0$** in THF (EF = 630 ± 30 nm) is not as large as that of **P1$_N$-BT$_{15}$** probably as a result of the higher fraction of ether linkages along the polymer chain and the ensuing better miscibility with the solvent.

Conclusions

Scheme 1 provides a method of synthesizing anionic CPs bearing carboxylate functionalities in good yield using established polymerization methods. The modular introduction of

(28) (a) Henry, B. R.; Morrison, J. D. *J. Mol. Spectrosc.* **1975**, *55*, 311. (b) Lin, T.-S.; Braun, J. R. *Chem. Phys.* **1978**, *28*, 379. (c) Lim, E. C. *J. Phys. Chem.* **1986**, *90*, 6770.
(29) Woo, H. Y.; Korystov, D.; Mikhailovsky, A.; Nguyen, T. Q.; Bazan, G. C. *J. Am. Chem. Soc.* **2005**, *127*, 13794.

fluorene units with either BT or substituted phenylene comonomers provides control over the content of lower energy sites along the polymer chain. The polymerization reaction yields precursor polymers $\mathbf{P1_N\text{-}BT}_x$ that are soluble in organic solvents and straightforward to characterize. Treatment of $\mathbf{P1_N\text{-}BT}_x$ with acid, followed by deprotonation with base, yields $\mathbf{P1\text{-}BT}_x$ polymers, which are negatively charged in basic media.

DLS results provide concrete evidence that changing the pH of **P1-BT$_0$** and **P1-BT$_{15}$** in water controls the degree of aggregation of these polymers. Large aggregates are observed when the pH is lower than ~3.7, the pK_a of the model compound HEPA. Under these conditions it is appropriate to consider these systems as colloidal suspensions. Increasing the pH results in aggregate breakup, most likely as a result of electrostatic repulsion between the negatively charge polymer chains; however, the resulting EDs are considerably larger than what would be expected on the basis of estimates for the molecular size of independent polymer chains (30−60 nm). Discrepancies of this type may arise from nonspherical aggregate and backbone shapes and the assumptions made in modeling the DLS data. From Figure 1 we observe that the general aggregation properties of **P1-BT$_{15}$** and **P1-BT$_0$** are nearly identical, consistent with the similarities in polymer structure ones and identical pendent functionalities.

Similarities in the absorption coefficients of **P1-BT$_0$** or **P1-BT$_{15}$** as a function of pH indicate that there is little or no precipitation, despite the large aggregate sizes. Comparison against the much lower solubility of related alkyl-containing or unsubstituted cationic fluorene−phenylene CPs highlights the importance of the oligo(ethylene oxide) groups in improving water solubility.[19] Figure 4 shows that in the case of **P1-BT$_{15}$** the absorption spectra are not perturbed by the state of aggregation, suggesting that there are no measurable changes in the degree of electronic delocalization in individual chains. That aggregation induces PL self-quenching in **P1-BT$_0$** and improved FRET to the BT units in **P1-BT$_{15}$** could perhaps have been predicted on the basis of enhanced interchain contacts, as shown by previous studies.[18,30,31] An important new observation is that the PL efficiency of the BT units in **P1-BT$_{15}$** solutions at low pH is considerably higher relative to conditions at high pH. Water induces quenching in the BT emission of $\mathbf{P1_N\text{-}BT_{15}}$ in THF. Since a similar quenching is not observed for $\mathbf{P1_N\text{-}BT_0}$ in THF, we conclude that this quenching is not due to interchain contacts. On the basis of these data we propose that aggregation of **P1-BT$_{15}$** at low pH reduces BT/water contacts and decreases energy-wasting nonradiative relaxation processes.

From the pH dependence of PL in Figure 6 we see that the responses of **P1-BT$_0$** and **P1-BT$_{15}$** occur over a narrow pH range, even though the mechanisms by which the emissions are modified are significantly different (PL self-quenching for **P1-BT$_0$** vs FRET and PL emission enhancement for **P1-BT$_{15}$**). Changes in PL appear to be sharper than the aggregation dependence on pH and suggest a higher level of cooperative response by the optical units than the aggregation of chains. It is also interesting that the inflection points in Figure 6 occur at a lower pH (~3.3) than the pK_a of HEPA. Such an effect would be expected when electrostatic repulsion between chains and aggregate breakup take place when a fraction of pendent groups are ionized.

In summary, we obtained new insight into how charge-mediated aggregation of conjugated polyelectrolytes influences the optical performance of the constituent units. Of particular significance is that the optical output can be increased within aggregates when the emitters are shielded from water contacts. The response of **P1-BT$_{15}$** has been shown to be reversible and, in contrast to standard single-molecule pH indicators, is a result of electrostatic interactions typical of polyelectrolytes in combination with the optical properties of conjugated polymers.

Experimental Section

General Details. ^{1}H and ^{13}C NMR spectra were collected on a Varian ASM-100 400 MHz spectrometer. UV−vis absorption spectra were recorded on a Shimadzu UV-2401 PC diode array spectrometer. Fluorescence was measured using a PT1 (Lawrenceville, NJ) Quantum Master fluorometer equipped with a Xenon lamp excitation source and a Hamamatsu (Japan) 928 PMT using 90° angle detection for solution samples. Mass spectrometry and elemental analysis were performed by the UC Santa Barbara Mass Spectrometry Lab and elemental analysis center. Reagents and chemicals were obtained from Aldrich Co. and used as received. Monomers **2**[21] and **3**[32] were synthesized according to reported procedures. Potentiometric titrations were performed with a glass/reference electrode, calibrated with buffer solutions of pH 4, 8, and 10. Titrations were performed using 0.1 N NaOH solution and a microburet to 10 mL polymer solutions under nitrogen at room temperature. Dynamic light scattering (DLS) was recorded using 10 mW HeNe laser (wavelength 633 nm) with photodiode detector BI-APD (Brookhaven Instruments Co.).

2,7-Dibromo-9,9-di(1-(2-(2-methoxy ethoxy)ethoxy)ethyl)fluorene. 1-(2-(2-Methoxy ethoxy)ethoxy)-2-bromoethane (55 g, 244 mmol) was added to a mixture of 2,7-dibromofluorene (7.9 g, 24.4 mol) and tetrabutylammonium bromide (TBAB) (0.78 g, 2.4 mmol) in 150 mL of aqueous KOH (45%) and heated at 60 °C for 4 h. After the reaction mixture was cooled to ambient temperature, the resulting solution was extracted with CH_2Cl_2 (3 × 100 mL). The combined organic fractions were washed with water, dilute HCl, and brine and dried over $MgSO_4$. The crude oily product was purified by chromatography on silica gel using a mixture of ethyl acetate and *n*-hexane (2/5) as the eluent to give 11.4 g (76% yield) of the product as a white solid: ^{1}H NMR (400 MHz, $CDCl_3$) δ (ppm): 7.53 (dd, 2H, J = 3.6 Hz, J = 1.6 z), 7.50 (s, 1H), 7.47 (dd, 2H, J = 8.0 Hz, J = 1.6 z), 3.53 (m, 4H), 3.49 (m, 4H), 3.39 (m, 4H), 3.35 (s, 6H), 3.21 (m, 4H), 2.76 (t, 4H, J = 7.6 Hz), 2.34 (t, 4H, J = 7.6 Hz). ^{13}C NMR (100 MHz, $CDCl_3$) δ (ppm): 151.0, 138.6, 130.8, 126.8, 121.8 121.4, 72.0, 70.6, 70.6, 70.2, 66.9, 59.2, 51.9, 39.6. MS (EI-MS) 616 (M). HRMS Calcd for $C_{27}H_{36}Br_2O_6$: 614.0879. Found: 614.0856.

2,7-Bis(4,4,5,5-tetramethyl-1,3,2-dioxaborolan-2-yl)-9,9-di(1-(2-(2-methoxy ethoxy)ethoxy)ethyl)fluorene (1). To a stirred solution of 2,7-dibromo-9,9-di(1-(2-(2-methoxy ethoxy)ethoxy)ethyl)fluorene (5.6 g, 9.1 mmol) in anhydrous THF (80 mL) at −78 °C was added dropwise *n*-butyllithium in hexane (7.6 mL, 2.5 M, 19 mmol) at −78 °C. The mixture was stirred for another 30 min, and 2-isopropoxy-4,4,5,5-tetramethyl-1,3,2-dioxaborolane (4.0 g, 21.5 mmol) was added rapidly at −78 °C. The reaction mixture was warmed to room temperature and stirred for another 24 h. The reaction mixture was poured into water and extracted with diethyl ether. The combined organic layers were washed with brine and dried over magnesium sulfate. The solvent was removed under reduced pressure, and the crude produce was purified by chromatography with 2/5 ethyl acetate and *n*-hexane to give 3.2 g of the product as colorless crystals (45% yield). ^{1}H NMR (400 MHz, $CDCl_3$) δ (ppm): 7.84 (s, 2H) 7.75 (dd, 4H, J = 7.6 Hz), 3.51 (m, 4H), 3.47 (m, 4H), 3.39 (m, 4H), 3.33 (s, 6H), 3.18

(30) (a) Fan, Q. L.; Zhou, Y.; Lu, X.-M.; Hous, Z.-Y.; Huang, W. *Macromolecules* **2005**, *38*, 2927. (b) Kim, B.-S.; Chen, L.; Gong, J.; Osada, Y. *Macromolecules* **1999**, *32*, 3964. (c) Kim, B.-S.; Fukuoka, H.; Gong, J. P.; Osada, Y. *Eur. Polym. J.* **2001**, *37*, 2499.
(31) Nguyen, T.-Q.; Schwartz, B. J. *J. Chem. Phys.* **2002**, *116*, 8198.

(m, 4H), 2.65 (t, 4H, J = 7.6 Hz), 2.44 (t, 4H, J = 7.6 Hz), 1.39 (s, 12H). ^{13}C NMR (100 MHz, $CDCl_3$) δ (ppm): 148.9, 143.6, 134.5, 129.7, 120.0, 84.4, 72.3, 70.9, 70.9, 70.4, 67.4, 59.5, 51.4, 40.0, 25.4. MS (EI-MS) 710 (M). HRMS Calcd for $C_{39}H_{60}B_2O_{10}$: 708.4445. Found: 708.4467.

General Polymerization Procedures. Polymerization reactions were carried out under palladium-catalyzed Suzuki cross-coupling conditions.[32] Carefully purified **1**, **2**, and **3** were mixed in the appropriate ratios with $(Ph_3P)_4Pd$ (1 mol %) in a mixture of 2 M Na_2CO_3 (aq) and toluene (1/1 v/v) under argon. After degassing, the reaction mixture was refluxed with vigorous stirring for 24 h. After cooling to room temperature, the organic layer was poured into methanol. The precipitate was separated by filtration and washed with methanol and acetone. Purification was accomplished by precipitation of toluene solutions into methanol. The neutral polymers were obtained by filtration and drying under vacuum. The obtained organic-soluble polymers are then dissolved in CH_2Cl_2, and an equal amount of trifluoroacetic acid was added. The mixture was then allowed to stir under argon at room temperature overnight. The solvent was removed under reduced pressured, and the residues were treated with saturated Na_2CO_3 (aq) solution for 4 h at room temperature. The reaction mixture was dialyzed in DI water to remove the salts. Solvent was removed, and the obtained solids were dried under reduced pressure overnight. The resulting polymers were soluble in water and methanol.

$P1_N$-BT_0. M_n = 56 054; M_w = 97 543, PDI = 1.74. Yield: 57%. ^{1}H NMR (400 MHz, $CDCl_3$) δ (ppm): 7.7 (4H), 7.6 (2H), 7.1 (2H), 4.2 (4H), 3.8 (4H), 3.7−3.6 (28H), 3.5−3.4 (16H), 3.3 (6H), 2.5 (4H), 1.4 (18H). ^{13}C NMR (100 MHz, $CDCl_3$) δ (ppm): 168.5, 148.1, 146.5, 136.8, 134.7, 128.7, 126.5, 121.9, 117.1, 114.4, 78.1, 69.4, 68.3, 68.2, 68.1, 68.1, 68.0, 67.9, 67.6, 67.4, 66.8, 64.9, 64.5, 56.6, 48.8, 33.8, 25.7. Anal. Calcd for $C_{59}H_{88}O_{18}$: C, 65.31; H, 8.11. Found: C, 64.86; H 7.98.

P1-BT_0. ^{1}H NMR (400 MHz, CD_3OD) δ (ppm): 7.9 (4H), 7.7 (2H), 7.2 (2H), 4.2 (4H), 3.8 (4H), 3.7−3.6 (24H), 3.5−3.4 (12H), 3.3 (14H), 2.4 (4H).

$P1_N$-BT_{15}. M_n = 25 702; M_w = 41 809; PDI = 1.62. Yield: 45%. ^{1}H NMR (400 MHz, $CDCl_3$) δ (ppm): 8.1 (1H), 7.9−7.7 (6H), 7.2 (1H), 4.2 (2H), 3.8 (4H), 3.7−3.6 (28H), 3.5−3.4 (16H), 3.3 (6H), 2.5 (4H), 1.4 (18H). ^{13}C NMR (100 MHz, $CDCl_3$) δ (ppm): 168.5, 151.7, 148.1, 146.5, 135.2, 134.7, 130.8, 128.7, 126.5, 125.7, 121.9, 117.1, 114.4, 78.1, 69.5, 68.3 68.3, 68.1, 68.1, 68.0, 67.9, 67.6, 67.4, 64.5, 49.0, 33.8, 25.7. Anal. Calcd for $C_{55.1}H_{80.5}N_{0.3}O_{16.2}S_{0.15}$: C, 65.46; H, 7.97. Found: C, 65.05; H 7.71.

P1-BT_{15}. ^{1}H NMR (400 MHz, CD_3OD) δ (ppm): 8.4 (0.5H), 8.0−7.7 (5H), 7.3 (1H), 4.3 (2H), 3.9 (4H), 3.8−3.6 (28H), 3.5−3.4 (16H), 3.3 (10H), 2.5 (4H).

Acknowledgment. This work was supported by the NIH (GM 62958-01) and NSF (DMR-0606414).

Supporting Information Available: ^{1}H NMR spectra of polymers **$P1_N$-BT_0**, **P1-BT_0**, **$P1_N$-BT_{15}**, and **P1-BT_{15}**, titration curve for HEPA, UV−vis spectrum of **P1-BT_0** film, and excitation spectra of **P1-BT_{15}**. This material is available free of charge via the Internet at http://pubs.acs.org.

JA065061X

(32) (a) Kitamura, C.; Tanaka, S.; Yamashita, Y. *Chem. Mater.* **1996**, *8*, 570. (b) Hou, Q.; Zhou, Q.; Zhang, Y.; Yang, W.; Yang, R.; Cao, Y. *Macromolecules* **2004**, *37*, 6299. (c) Huang, J.; Niu, Y.; Yang, W.; Mo, W.; Yuan, M.; Cao, Y. *Macromolecules* **2002**, *35*, 6080.